Polym. Bull. (2018) 75:1789–1807
https://doi.org/10.1007/s00289-017-2123-y

ORIGINAL PAPER

Nanocomposites foams of poly(ethylene-*co*-vinyl acetate) with short and long nanocellulose fibers and foaming with supercritical CO_2

Matheus V. G. Zimmermann[1] · Ademir J. Zattera[2] · Ruth M. C. Santana[1]

Received: 28 April 2017 / Revised: 12 June 2017 / Accepted: 8 July 2017 /
Published online: 15 July 2017

Abstract Nanotechnology applied to polymer foams is an emerging field, because even at low filler contents, different cellular morphologies can be obtained in the development of foams. Based on these premises, this work addresses the development of poly(ethylene-co-vinyl acetate)—EVA foams reinforced with two types of nanocellulose (a) short fibers (NC), and (b) long fibers (NCF). The foams were expanded in an autoclave with supercritical carbon dioxide (CO_2). Different expansion conditions were evaluated, with variations of temperature and pressure. The main results indicate that the presence of the fibers significantly reduces the size of the cells and increase the number of cells per unit area. However, by increasing the NC content, nanocellulose fibers agglomeration is observed, resulting in the formation of a bimodal cellular structure.

Keywords EVA · Foams · Supercritical fluids · Cell nucleation · Cellulose

Introduction

Polymeric foams, cellular polymers or expanded polymers have at least two phases. One of them is the solid phase, which consists of a polymer matrix and the other is the gas phase, which is the distribution of porous nuclei generated by the action of gases from a foaming agent. These foams are materials formed by air bubbles

✉ Matheus V. G. Zimmermann
matheus.vgz@gmail.com

[1] Graduate Program in Mining, Metals and Materials Engineering (PPGE3M), Federal University of Rio Grande do Sul (UFRGS), Porto Alegre 91501-970, Brazil

[2] Graduate Program in Process and Technology Engineering (PGEPROTEC), University of Caxias do Sul (UCS), 95070-560 Caxias do Sul, Brazil

dispersed in a polymer matrix, which are called cells. By the presence of a porous system, polymer foams are, in general, materials with reduced density in comparison to their primary constituent (polymer) [1, 2].

The development of polymer foams is based on the incorporation of an expanding agent (or foaming agent) into a polymer matrix. This foaming agent may be physical or chemical. The first generally consists of low boiling liquids which volatilize during processing, while the latter are solid chemical compounds that decompose with increasing temperature, generating gases such as nitrogen (N_2) and carbon dioxide (CO_2) [3–5].

Physical blowing agents cause no chemical change in the material, only a change of state, and the final nature of the blowing agent must be in the gaseous form to promote the formation of air bubbles within the polymer matrix. The phase change of a physical blowing agent can occur either by the volatilization of a liquid, or by the decompression to atmospheric pressure of a compressed gas [2].

In recent years, polymer foam processing industry has experienced serious regulatory, environmental and economic pressures due to the use of toxic and environmentally hazardous foaming agents, such as chlorofluorocarbons (CFCs), banned in the industry. Thus, the use of supercritical fluids for the production of polymer foams has become prominent. In this context, mainly carbon dioxide (CO_2) has been used as a physical foaming agent for the production of polymeric foams.

Supercritical fluids are defined as substances in which the pressure and temperature of the material are above the critical point where there is no further distinction between the liquid and gaseous phases. In general, the use of supercritical fluids offers advantages over conventional physical expanders, such as greater solubility due to its gas-like diffusivity, liquid-like density, low viscosity and surface tension [6]. Their main representative is the carbon dioxide (CO_2).

The main advantage in using CO_2 is the low pressure and temperature required to reach the critical point as opposed to other materials. The CO_2 supercritical condition is possible through compression (critical pressure = 73.6 bar) and heating (critical temperature = 31.1 °C). After decompression to atmospheric pressure, CO_2 is released into the gas phase without any condensation. Furthermore, CO_2 is a non-toxic material with a high solubility in most polymers, with a great variation in the solubilization capacity according to process conditions, low cost and solvent recycling capacity for later reuse, which are advantages in using it in the supercritical state as a foaming agent in polymer foams. In addition, the low critical temperature of carbon dioxide allows easy and complete separation of the polymer, without the occurrence of a liquid–vapour transition, during expansion, which may result in the contraction of foam cells [7]. Liquid–vapour transition during expansion promotes the contraction of the cell by condensation of the fluid, which in the cooling generates vacuum inside the cell, preventing its growth, and deforming its structure [8].

Several polymeric foam expansion methods have been developed with the use of supercritical fluids. Among these methods, extrusion [6] and the use of autoclaves stand out [7]. In the expansion by batch process, using autoclaves, the polymer is saturated with a gas (usually CO_2), and then the system is brought to the supersaturated state (supercritical gas condition) with constant temperature and

pressure. Then, by reducing the pressure (pressure induced by phase separation) or by increasing the temperature (induced phase separation temperature) nucleation and growth of the cells and pores within the polymer matrix are promoted [9, 10].

With the advent of the development of polymeric foams with supercritical gases or fluids, a wide range of cellular structures can be developed in the foams, especially the production of microcellular polymers [9]. Due to the small size of the cells present in the microcellular foam structure, their mechanical properties often resemble a non-expanded compact polymer, with the advantage of being a material of reduced density.

In addition, the formation of polymeric foams with supercritical fluids has a great advantage in the processing of polymers for biomedical applications, such as scaffolds [11]. In this process, no organic solvents and chemical compounds that are harmful or toxic to organisms are needed. In most cases, these compounds are not easily removed from the final product, requiring several steps of material sterilization [9].

Several studies report the advantages in using nanofillers and nanofibers in expanded composites or reinforced polymer foams using supercritical fluids [10, 12–14]. The development of foams with nanocomposites is one of the most recent evolutionary technologies of polymer foams. Nanocomposite foams offer an attractive potential for the diversification and application of conventional polymeric materials. The fact that nanofillers induce a high heterogeneous nucleation of the cells allows the morphology of the cells of the foam to be modified by low contents of fillers. Cells of diverse sizes can be produced, with cell sizes ranging from micro to nanometric [10].

Currently most widely used nanofillers in the formulation of polymer foams consist of inorganic materials. Recently, however, organic materials such as cellulose nanofibers, have been attracting attention for being less abrasive and lighter than inorganic materials [15]. The term nanocellulose generally refers to cellulosic materials in which at least one of the dimensions of the fiber must be nanometric. Cellulose nanostructures from vegetable sources are classified into two main categories based on their dimensions, applications and methods of preparation: (a) cellulose nanofibers (NCF—long fibers) and (b) cellulose nanocrystals (CN—short fibers) [16, 17].

In general, CN have elongated filaments and limited flexibility, because they have no amorphous regions, and low aspect ratio (width/diameter). They are generally obtained by chemical treatments, such as acid hydrolysis, with or without the association of mechanical processes and have diameters from 2 to 20 nm and a length from 100 nm to several micrometers. NCF are classified as the smallest structural part of the vegetal fiber, composed of a set of cellulose molecules with long length, high flexibility and entanglement capacity. They have, in general, diameters below 100 nm, with variable lengths and intercalation of amorphous and crystalline regions. They are usually obtained by mechanical processes [18, 19].

In general, the presence of fibers and fillers affects the nucleation kinetics of the polymer foam cells during expansion. Cell nucleation is a term assigned to any process that leads to the formation of a bubble in the polymer matrix. Considering that a polymer melt is already fully saturated with an expansion agent, with a phase

change, either by induction of temperature or pressure, the system becomes supersaturated. Therefore, the gas polymer solution tends to form small bubbles in order to restore a stable low energy state. The theory of classical cell nucleation in polymer materials classifies cell nucleation into two types—homogeneous and heterogeneous nucleation, as shown in Fig. 1 [1, 20–22].

In homogeneous nucleation, with the phase change, air bubbles are formed spontaneously and randomly inside the polymer matrix. When a bubble reaches a critical size, other smaller-sized bubbles tend to migrate to this region, coalescing and propagating the size from this unit. In addition, it is also believed that the phase change also causes small voids in the polymer matrix, which favors the migration of the gas from the expander to this region.

In heterogeneous nucleation, the gas is dispersed in a heterogeneous environment, with at least two distinct phases. Among the heterogeneous elements attributed to this theory, the use of fillers, different polymer matrices and also crystals (in the case of semicrystalline polymers) stand out. During cell formation, the gas tends to migrate to the lower energy region. In a heterogeneous system, the lower energy region is preferably in the region of the interface, that is, in the contact area of the system, for example, polymer–filler. The manipulation of this interface region, either by the content or the size of the filler, may impact on the varation of the cellular morphology of the foam in formation [22].

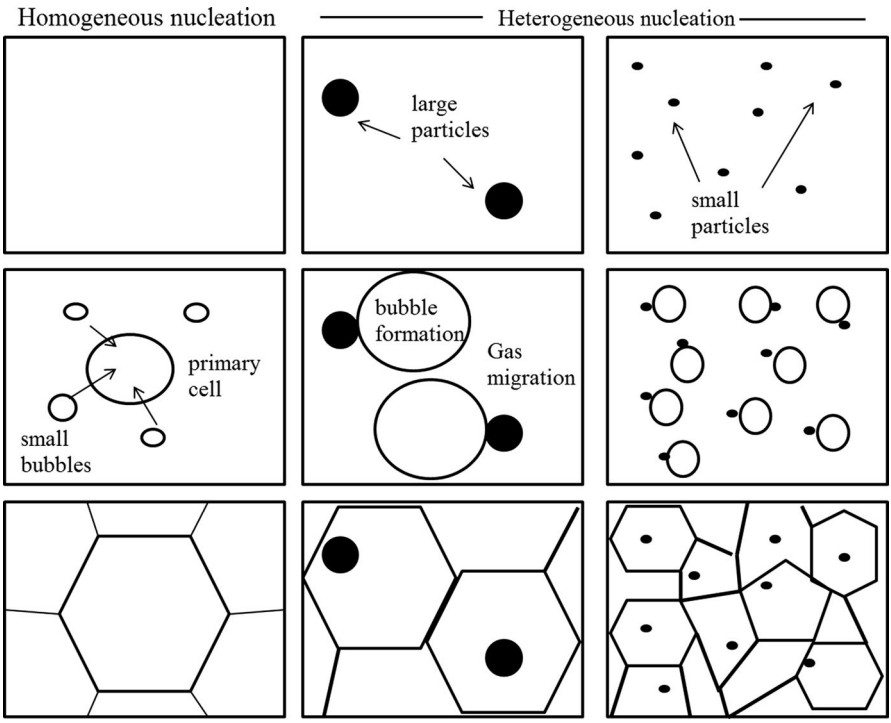

Fig. 1 Homogeneous and heterogeneous cell nucleation in a polymeric foam

In the production of polymeric foams using supercritical fluids as a blowing agent, various parameters may influence the final morphology of the foam. Among the main associated factors are: polymer viscosity, polymer transition temperature (glass transition temperature and melting), processing variables such as pressure and temperature, time of exposure of the sample to the supercritical fluid, depressurization rate (time to remove the supercritical fluid from the system) as well as the presence of fillers [10].

Materials and methods

Materials

The EVA copolymer (trade name EVATENO 3019 PE) was provided by Braskem S.A. It contains 19% of vinyl acetate and density of 0.940 g/cm^3, melt flow rate (MFR) (190 °C/2.16 kg) of 2.5 g/10 min and a melting temperature of 86 °C.

Two types of cellulose fibers were used in this study: microcrystalline cellulose (MC) supplied by Sigma-Aldrich, named Sigamacell-20 (cod. S3504), with an average diameter of 20 μm (short fiber) and Bleached cellulose fibers (CF) (long fiber), obtained from eucalyptus trees, provided by Celulose Riograndense S.A. (Brazil/RS). The cellulose pulp was acquired in the form of sheets. Before its use, it was ground in a MARCONI knife grinder, with a Ø 1 mm sieve.

Methods

MC and CF were mechanically defibrillated in a super mass colloider grinder (MKCA6-2, Masuko Sanguo). MC was ground using a suspension containing 4.5 wt% of MC in distilled water to obtain short cellulose nanofibers (NC). CF was ground in a solution with water and 3 wt% of cellulose to obtain nanocellulose long fibers (NCF). The equipment was coupled to a recirculating pump and the grinding time was 4 h at a speed of 2000 rpm. The ultrafine-milling mechanical process consists in breaking the cellulose wall structure due to shear forces generated by the grinding stones from the mill (usually non-porous resins containing silicon carbide). To perform the fibrillation in mills, cellulose fibers at low concentrations are dispersed in water, and the suspension is forced to pass between two wheels/stones, one rotating and the other static. The use of water as a base medium helps the swelling of the cellulose fibers and thereby facilitates the breaking of hydrogen bonds between the cellulose cell walls. The contact surfaces and the grooves of the stones along with the repeated cyclic stresses result in the defibrillation of cellulose [23, 24].

After grinding, both cellulose suspensions were centrifuged using a centrifuge Novatecnica, NT820 model, at a speed of 5000 rpm, during 30 min. The phases were separated and the solid/water relation was measured and stabilized to a solids ratio of approximately 20% for NC and 10% for NCF.

Figure 2 shows the TEM micrographs of NC and NCF in which the diameter of the fibers is in nanoscale in both samples.

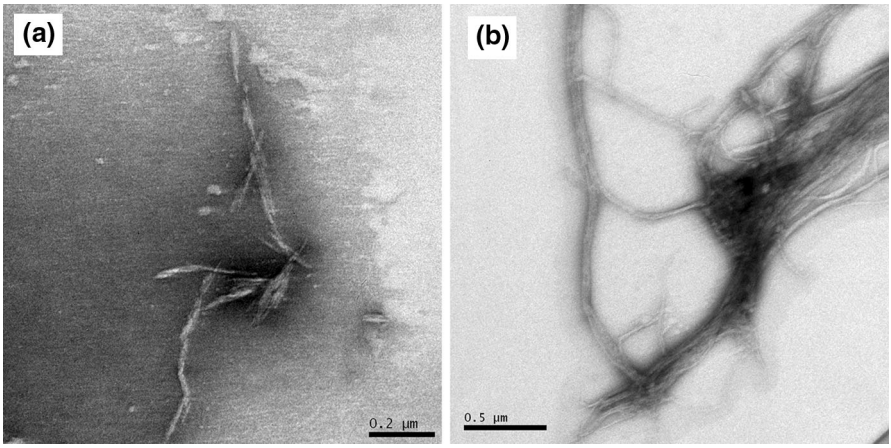

Fig. 2 TEM microscopy of the cellulose fibers after grinding **a** NC and **b** NCF

The incorporation of the CN and NCF suspensions in the EVA was carried out in a mixing chamber (torque rheometer) at a temperature of 120 °C with a rotor speed of 100 rpm during 600 s. The cellulose was added to the EVA at concentrations of 1, 2 and 3%. The dispersant additives added to the cellulose suspension with high solids content were the following: 1 g of oil (Olvex 51), 1 g of n-heptane and 1 g of surfactant (Niax Silicone L-595) to facilitate dispersion during the incorporation of both nanocelluloses. The content of the additives was kept constant regardless of the cellulose content added to the polymer. The cellulose suspension was added dropwise during the processing period. Subsequently, the material was pressed into a 2-mm plate using a thermal press (SCHULZ) at 120 °C, with 5 ton for 2 min. The plates were placed in a thermal oven with vacuum at 60 °C for 24 h to promote the oil migration to the composite surface.

The expansion process of the EVA foams was carried out using CO_2 in supercritical state as the foaming agent, in equipment from Supercritical Fluids Technologies SFT, model SFE 150 (Fig. 3), with 1-L pressure vessel. A volume

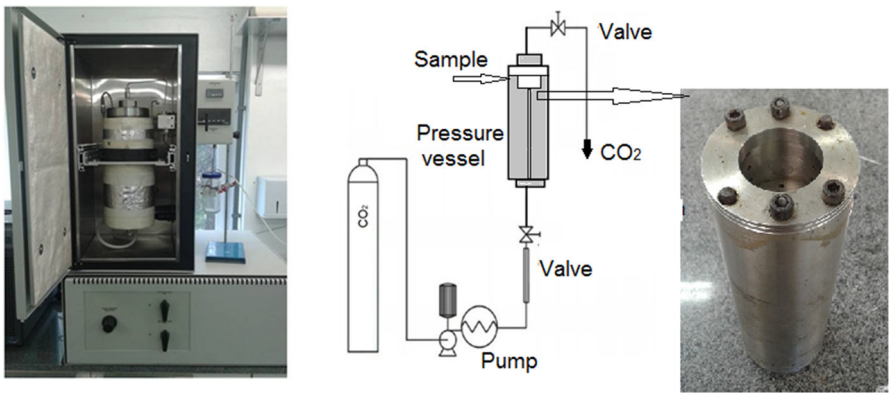

Fig. 3 Equipment used for the expansion of EVA foams and the volume reducer

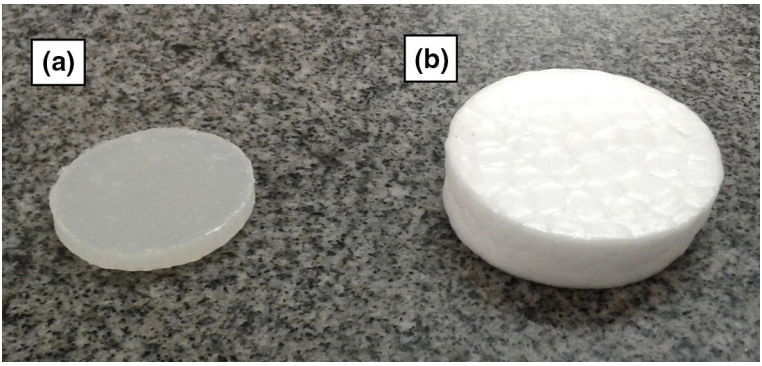

Fig. 4 **a** Preform and **b** EVA foam expanded with supercritical CO_2 produced at 80 °C and 2400 psi

reducer was used in the pressure vessel to decrease the volume to 200 cm^3. The conditions of temperature and pressure expansion were varied, while the residence time of the specimen in the pressurized vessel, 2 h, was kept constant. The system depressurising time of 3 min was also kept constant.

Figure 4 shows the photographic image of the preform used (Fig. 4a) and its EVA foam (Fig. 4b), produced in a pressure condition of 2400 psi and temperature of 80 °C.

Characterizations

After mechanical defibrillation, the cellulose was evaluated by transmission electron microscopy (TEM) using the Jeol Jem 2010 equipment. Uranyl acetate was used as contrast and the analysis was applied at a voltage of 120 kV.

The rheological properties of the EVA/cellulose composites in the molten state were evaluated by capillary rheometry using the equipment Instron, model 4204, according to ASTM D3835-93. The viscosities of the blends were evaluated at shear rates of 100–3000 s^{-1} using a capillary of $D = 1$ mm and $L = 20$ mm at a temperature of 120 °C. The Rabinowitsch correction was used to adjust the Newtonian behavior deviation.

Dynamic mechanical analysis (DMA) was performed on EVA/cellulose composites, prior to expansion, in a device from TA Instruments, model DMA T800. The dual cantilever method was used, with a heating rate of 3 °C min^{-1} within the temperature range of −60 to 60 °C, frequency of 1 Hz and strain amplitude of 0.1%.

The apparent density of the EVA foams was calculated by the mass (g) and volume (cm^3) ratio. The method was performed according to the standard ASTM D1622-08. The measurements were carried out in 5 samples for each formulation, in different parts of the expanded foam.

The morphology of the fractured surface of the foams was evaluated by scanning electron microscopy (SEM) using the equipment Tescan Mira3. All samples were previously coated with Au. The observation area in all foams was analyzed in cross

section (horizontal direction) of the expanded sample. The software used to measure the cell size was ImageJ. The cell population density per unit volume of the foamed composites (N_f) was determined from the SEM micrographs using Eqs. (1) and (2) [25, 26]

$$V_f = \left(1 - \left(\frac{\rho_f}{\rho_p}\right)\right), \tag{1}$$

$$N_f = \left(\frac{nM^2}{A}\right)^{3/2} \cdot \left(\frac{1}{1 - V_f}\right), \tag{2}$$

where V_f *i*s the void fraction (%), ρ_f is the density of the foam (g cm^{-3}), ρ_p is the unfoamed polymer density (g cm^{-3}), N_f is the cell density (cell cm^{-3}), A is the area of the micrograph (cm^2), M is the magnification factor for micrograph, n is the number of bubbles in the SEM micrograph (cells). The cell size was measured by the Ferret diameter.

The thermal properties were evaluated using differential scanning calorimetry (DSC) in a SHIMADZU model DSC-60 instrument at a heating rate of 10 °C min^{-1} and scanned from 0 to 200 °C with a 3-min isotherm. The crystallinity index (X_c) was calculated from the second heat, according to Eq. 3:

$$X_c(\%) = \frac{(\Delta H_m)}{(\Delta H_o) \times w} \times 100, \tag{3}$$

where ΔH_m is the melting enthalpy of the sample (J/g), and ΔH_o is the melting enthalpy for 100% crystalline EVA, which corresponds to 293 J/g and w is the X_c correction by the EVA content in the compound.

Results and discussion

Characterization of EVA nanocomposites with cellulose (NC and NCF)

Figure 5 shows the rheological properties of NC and NCF-reinforced EVA in molten state, at 120 °C. No significant changes were observed in the rheological properties with the insertion of the cellulose nanofibers. In other words, there were no significant changes in the viscosity of the polymer in the molten state, a parameter that can directly affect the expansion capacity of the foams. Figure 5 shows that only at low shear rates, the nanostructured samples with cellulose presented a slight decrease in relation to pure EVA, which was more evident in the NC-reinforced sample. This decrease may be due to the cellulose fibers acting as lubricants of the polymer chains, which causes a low reduction on the matrix viscosity of the polymer. The presence of nanofibers between EVA molecules as well as fiber agglomerates may decrease the interaction forces of the molecules, especially in the molten state, which leads to a slight decrease in strength and a decrease in viscosity.

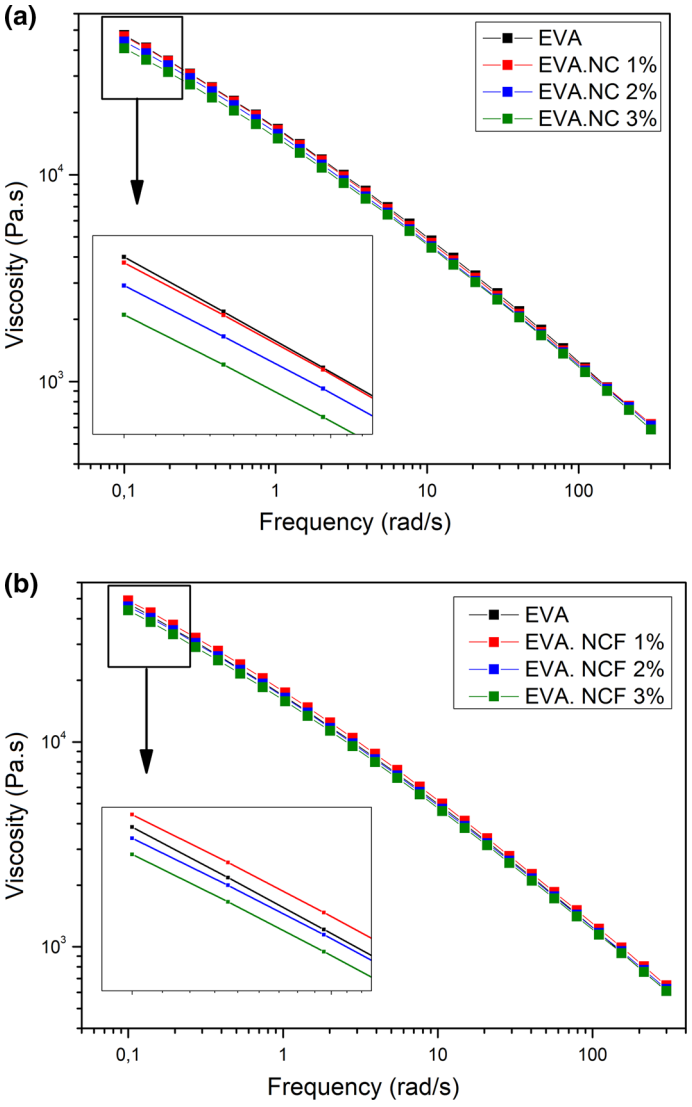

Fig. 5 Rheological properties of EVA composites with: **a** EVA composites with different NC contents and **b** EVA composite with different NCF content

Figure 6 shows the viscoelastic behavior of EVA and EVA composites (non-expanded) with long and short cellulose nanofibers, obtained by DMA. Figure 6a and b show the overlapping curves of the storage modulus, where it is possible to visualize the differences in elastic response at low temperatures in the glassy region. The nanocomposites presented a higher modulus than pure EVA, mainly in the composites produced with 1% of NCF. At low temperatures, EVA.NC composites presented lower values of storage modulus than EVA.NCF 1% and EVA.NCF 2% composites, and this difference decreases in the temperature of use (0–30 °C).

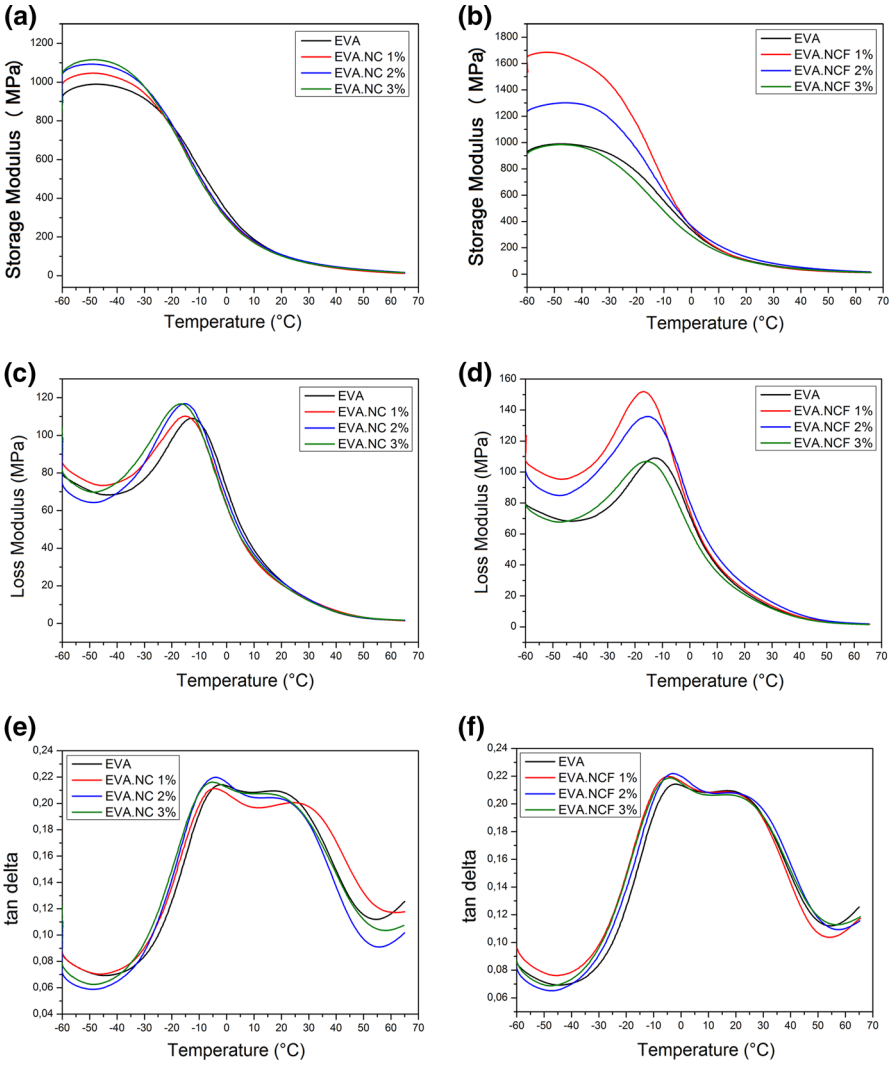

Fig. 6 Dynamic-mechanical properties of EVA composites prior to expansion with **a**, **c** and **e** NC and **b**, **d** and **f** NCF

Figure 6c and d show the overlapping curves of the loss modulus of the evaluated samples, where it is possible to detect a slight decrease in the glass transition temperature of EVA with the presence of the fillers. Figure 6e and f show the overlapping curves of mechanical damping, known as Tan delta, and where it is possible to observe that EVA has two distinct relaxation events, the first happens around −5 °C and is attributed to α-relaxation of the ethylene fraction. The second, near 25 °C, is attributed to α-relaxation of vinyl acetate. According to Sefadi and Luyt [27], the first α-relaxation is due to the movement of chain segments of three or four methylene groups (–CH_2–) and is associated to the glass transition of the

material (T_g). Below the T_g, the segments of the molecular chains are frozen and the damping is low. Consequently, little energy is stored in the elastic deformations. In the rubbery region, the damping is higher compared to the glassy state because the molecular segments are free to move, which results in decreasing stiffness, and dissipation of excess energy as heat. The second α-relaxation may be related to the movement of the amorphous regions within the crystalline phase, namely, the reorientation of defect regions between the crystals, or also attributed as a reflection of the relaxation of the flexible chains of the vinyl acetate groups present in EVA copolymer chains [27].

Characterization of EVA foams produced under different processing conditions

Firstly, the influence of temperature on the expansion of pure EVA using supercritical CO_2 was evaluated. In the processing of EVA foams, only the melt temperature is of interest during the process because the glass transition temperature is well below the processing temperature [7].

Figure 7 show the micrographs obtained by SEM and Table 1 the foams characteristics. They present the variation of the morphologies of the pure EVA foams, and the characteristics of the EVA foams produced with temperatures of 40, 80 and 120 °C, at a constant pressure (2400 psi). It is observed that by increasing the temperature of the system, the tendency of formation of larger cells is higher. According to Tsivintzelis et al. [9], when the CO_2 foam saturation occurs at higher temperatures, CO_2 diffusivity is also increased, making cell growth more pronounced. In addition, the saturation and solidification pressure range is increased, resulting in longer periods of exposure of the sample to high temperatures, resulting in the formation of larger cells and foams that have, in general, reduced densities. As the temperature increases, the viscosity of the polymer matrix also decreases and consequently the decrease in the resistance of the molten polymer will withstand the action of the gases. With the decrease of viscosity, there is a greater propensity to coalescence of cells, with formation of larger cells and in some cases deteriorated or with pores (open cells) [7].

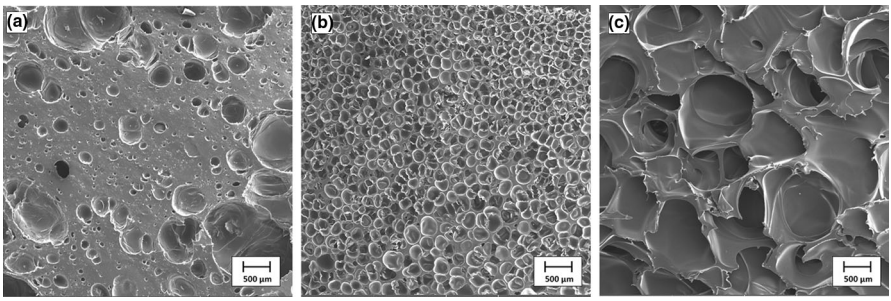

Fig. 7 EVA foams, produced at constant pressure (2400 psi) and temperature variation **a** 40 °C; **b** 80 °C and **c** 120 °C

Table 1 Characteristics of EVA foams produced under different temperature conditions (40, 60 and 120 °C) and constant pressure (2400 psi)

Temperature at which the foam was produced (°C)	Foam density (g/cm^3)	Porosity (%)	Average cell size (μm)	Cell number per micrograph*	*Nf* (cell/cm^3)
40	0.54 ± 0.06	42.5	162 ± 125	82	1.45×10^7
80	0.19 ± 0.01	79.7	222 ± 69	246	1.41×10^8
120	0.21 ± 0.01	77.0	548 ± 82	22	3.68×10^6

* SEM magnification = 100×

The influence of temperature on the foam morphology is relatively complex, because the temperature variation has a direct influence on the level of gas diffusivity within the polymer, on the nucleation rate and on the viscosity of the polymer [7]. In foams produced at a temperature of 120 °C, a distinct deformation of the cells can be observed, with possible coalescence and pore opening, as this process is carried out at temperatures above the EVA melting temperature, which is 86 °C according to the manufacturer of the material. In this situation, it is very difficult to control the reproducibility of the geometry of the produced foams, given the instability of the polymer matrix at this temperature. In foams produced at a temperature of 40 °C, less cells are formed per unit area in relation to the other foams. In foaming processing using semicrystalline polymers, which is case of the EVA copolymer with 18% vinyl acetate, gas diffusivity occurs preferentially and primarily in the amorphous regions of the polymer, and in this sample, as the processing temperature is below the melting temperature, the cell nucleation occurs in the amorphous segments. The foam produced at the temperature of 80 °C shows the formation of a structure of homogeneous sized cells, with an average cell size of 100–200 μm, which was assigned to this experimental as the ideal temperature for this sample.

For a better understanding of the thermal properties of EVA, the DSC thermograms of EVA and EVA composites with NC are shown in Fig. 8. The EVA fusion event starts at 77 °C, has the maximum reaction intensity (T_m) at 90 °C and the end of the event near 97 °C. During cooling, the crystallization of the polymer occurs in the temperature range of 70 to 57 °C. The crystallinity of pure EVA is 10.6%.

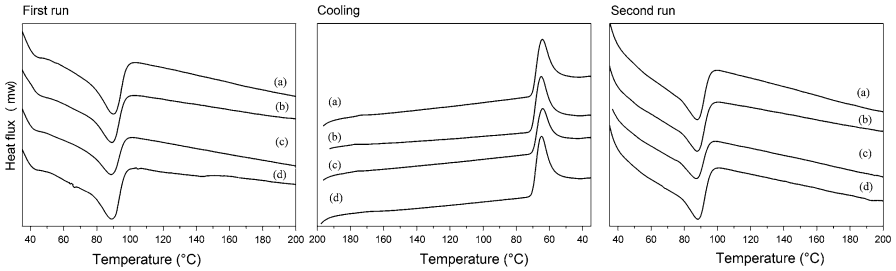

Fig. 8 DSC thermograms of **a** EVA and EVA composites with different NC content: **b** 1%; **c** 2% and **d** 3%

According to Xu et al. [28], it is much more difficult to control the cellular structure of a foam in semicrystalline polymers than in fully amorphous polymers. The gases do not dissolve in the crystalline regions and the polymer/gas solution formed during the process is not uniform because it does not have a homogeneous nucleation in the crystalline and amorphous phases. Thus, foams in semicrystalline polymers should preferably be expanded at temperatures close to or above the melting temperature. Another strategy to control cell size stability in semicrystalline polymers is in the use of fillers and nanofillers. Considering that these fillers act as nucleation points for cells, the influence on the type of nanocellulose (long and short fibers) was evaluated, as well the variation of the concentration of these fibers.

Figure 9 presents SEM micrographs of the morphology of foams with the insertion of short cellulose fibers at constant temperature and pressure of 80 °C and 2400 psi, respectively. Figure 10 shows the foams produced with long fibers. Table 2 shows the characteristics of the foams.

Figure 7b shows that in the comparison of the pure EVA micrograph, the presence of the cellulose fibers causes a decrease in the size of the cells and an increase in the number of cells per micrographs in relation to the pure EVA foam.

Cell density is affected both by the content and the size/diameter of the filler. In general, the presence of fillers acts as nucleation points for the cells, considering that the existence of micropores or voids in the polymer–filler interface provides the

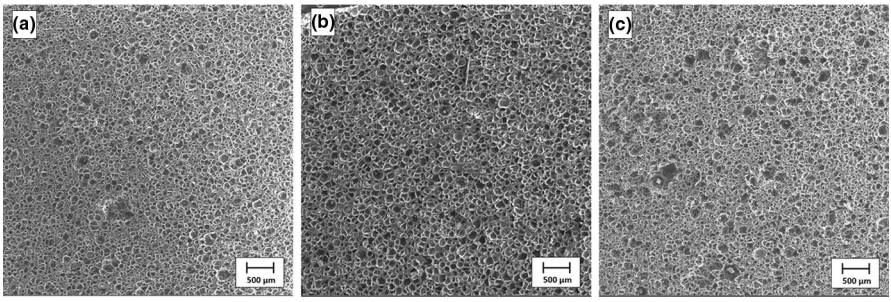

Fig. 9 EVA foams produced with constant pressure (2400 psi) and constant temperature (80 °C) and variation on NC content: **a** 1%; **b** 2% and **c** 3%

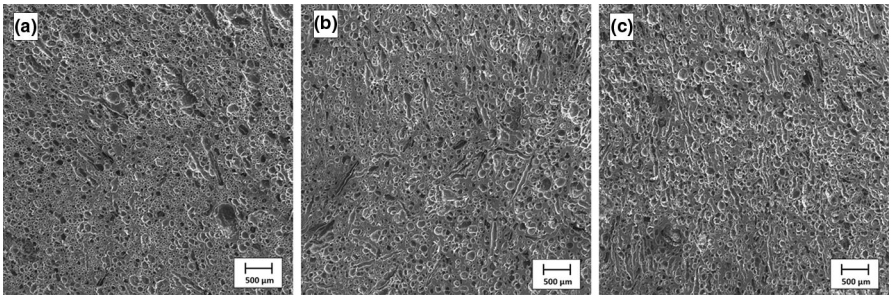

Fig. 10 EVA foams with constant pressure (2400 psi) and constant temperature (80 °C) and variation on NCF content: **a** 1%; **b** 2% and **c** 3%

Table 2 Characteristics of EVA foams reinforced with NC and NCF, produced with constant temperature (80 °C) and constant pressure (2400 psi)

Sample	Foam density (g/cm^3)	Porosity (%)	Average cell size (μm)	Cell number per micrograph*	*Nf* (cell/cm^3)
EVA/NC1	0.168 ± 0.009	82.0	109 ± 25	1086	1.35×10^9
EVA/NC 2	0.174 ± 0.005	81.0	96 ± 20	954	1.10×10^9
EVA/NC 3	0.200 ± 0.002	78.0	156 ± 73	836	8.74×10^8
EVA/NCF 1	0.264 ± 0.017	71.9	80 ± 50	912	9.15×10^8
EVA/NCF 2	0.297 ± 0.020	68.4	98 ± 47	948	9.17×10^8
EVA/NCF 3	0.318 ± 0.020	66.0	175 ± 94	567	4.10×10^8

* SEM magnification = 100×

migration of the generated gas to these regions, thus promoting the propagation and growth of the cell starting in this site [Trone, 1996]. As the fiber size decreases, the contact area of the fibers with the polymer matrix increases, which may lead to the formation of a larger number of sites for cell nucleation.

According to Chen et al. [29], larger particles contain more trapped air (greater contact area) and promote the formation of larger cells. As the particle size decreases and the content remains constant, there is a higher concentration of smaller fibers and, consequently, a larger number of cells is formed (increase in cell density) compared to larger particles.

However, with increasing CN content, an increase of large cells is observed and in the contour of this large cells the presence of a large amount of small cells is observed. The presence of two distinct cell groups (two sizes) is defined as a bimodal foam, as discussed by Duang et al. [30].

As mentioned previously, cellulose nanofibers act as nucleating agents for the formation of cells, but if during the incorporation of the fiber to the polymer matrix, agglomeration and aggregation of fibers occurs, the coalescence of cells and formation of larger cells is favored. A higher interface (contact area between the fiber and the polymer matrix) favors the formation of larger cells because the gas from the expander tends to migrate to the region of least resistance, and propagate its growth from this point. Thus, with the effect of dimorphism on the size of the nanometric and agglomerated particles, the formation of a bimodal foam is favored, and with the increase of the cellulose fibers, the probability of obtaining agglomerated fibers is greater. Consequently bimodal foams are more likely to occur [30].

Figure 11 shows the micrographs of the cellular structure of the EVA.NC composite. The dispersion of the NC in the cellular structure of the EVA foam is presented. Individualized fibers present in the EVA.NC 1% composite and agglomerated segments in the EVA.NC 3% composite can also be observed.

Figure 12 shows the micrographs of the cellular structure of the EVA.NCF composite. The distribution of the NCF in the cellular structure of the EVA foams is shown. In addition, the figure presents the clear formation of cells that are formed in

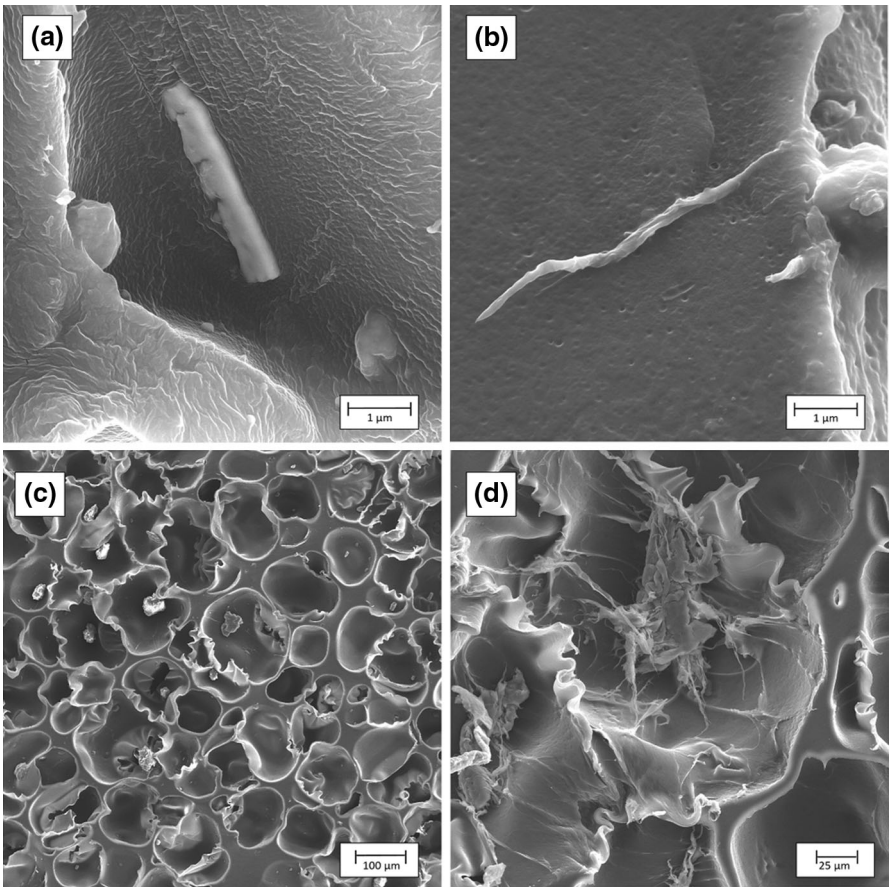

Fig. 11 Micrographs obtained by SEM, showing the dispersion of NC in the cellular structure of EVA foams in **a**, **b** EVA.NC 1% and **c**, **d** EVA.NC 3%

the contour of the long cellulose fibers, promoting the formation of a large amount of non-spherical cells.

Another variable of great influence in the modification of the cell morphology in polymer foams produced with supercritical fluids is the pressure used in the system. Figure 13 shows SEM micrographs of EVA foams reinforced with 1% of NC, produced at a constant temperature (80 °C) and pressure variation. Data relating to the foam characteristics are presented in Table 3. The cell size tends to decrease with increasing pressure and concomitant to this increase. In addition, foams with bimodal cells (with two cell sizes) tend to be formed with increasing pressure. According to Jacobs et al. [7], the growing saturation of the system by CO_2, leads the cell to collapse, forming cells of different sizes.

In the classical theory of cell nucleation in polymer foams, the nucleation rate, i.e., the number of cells formed per unit time and volume, can be expressed as a

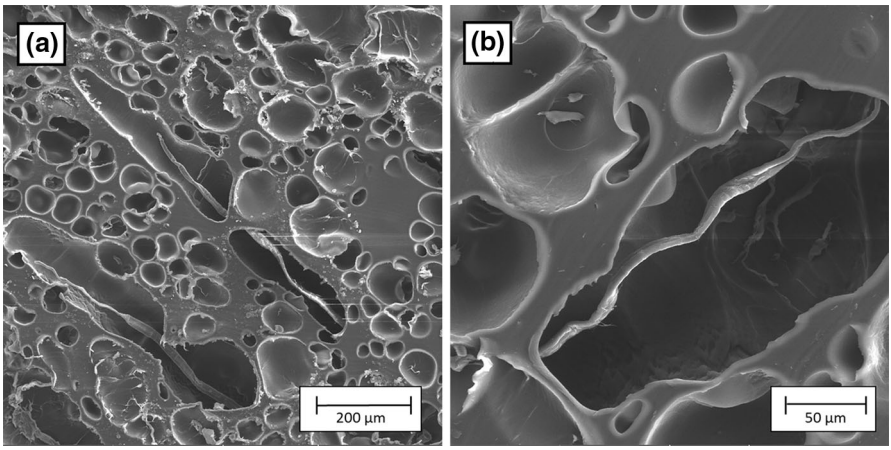

Fig. 12 SEM Micrographs of EVA foams reinforced with long cellulose fibers, at different magnifications: **a** 300× and **b** 1000×

function of the Gibbs free energy barrier for the formation of a nucleus for the formation of a cell. The theory suggests that the energy barrier and interfacial tension decrease with increasing supersaturation pressure. Thus, with increasing pressure, the nucleation rate increases and a greater amount of cells is formed. Thus, by controlling the amount of supercritical CO_2 during foam processing, it is possible to modify the cell density size in the foam [6, 31].

Conclusions

By analyzing the EVA composites with cellulose nanofibers, no significant variations were observed in the rheological and thermomechanical (at room temperature) properties with the fiber insertion, which suggests that these fibers act only as nucleating agents, not reinforcing agents. In the production of polymer foams, the use of supercritical fluids is an alternative of great potential, since it allows, with simple adjustments in the processing conditions, to obtain varied cellular morphological structures, and concomitantly, different properties can be conferred to the foams. The use of nanofillers helps in the formation of cells, as they act as heterogeneous sites for nucleation and growth of cells during expansion. In general, the use of cellulose short fibers promoted a greater homogeneity of cell. However, with increasing the content, coalescence and deformation of the cell structure of the foam by the agglomeration of the fibers occurs, with the formation of bimodal cellular structures. In the use of long cellulose fibers, we observed cell growth along the entire fiber contour, which leads to the production of non-spherical cells, that is, a large heterogeneity in cell size, mainly impacting the expansion capacity and density of the foam. The saturation pressure also influences the modification of the cellular structure: the

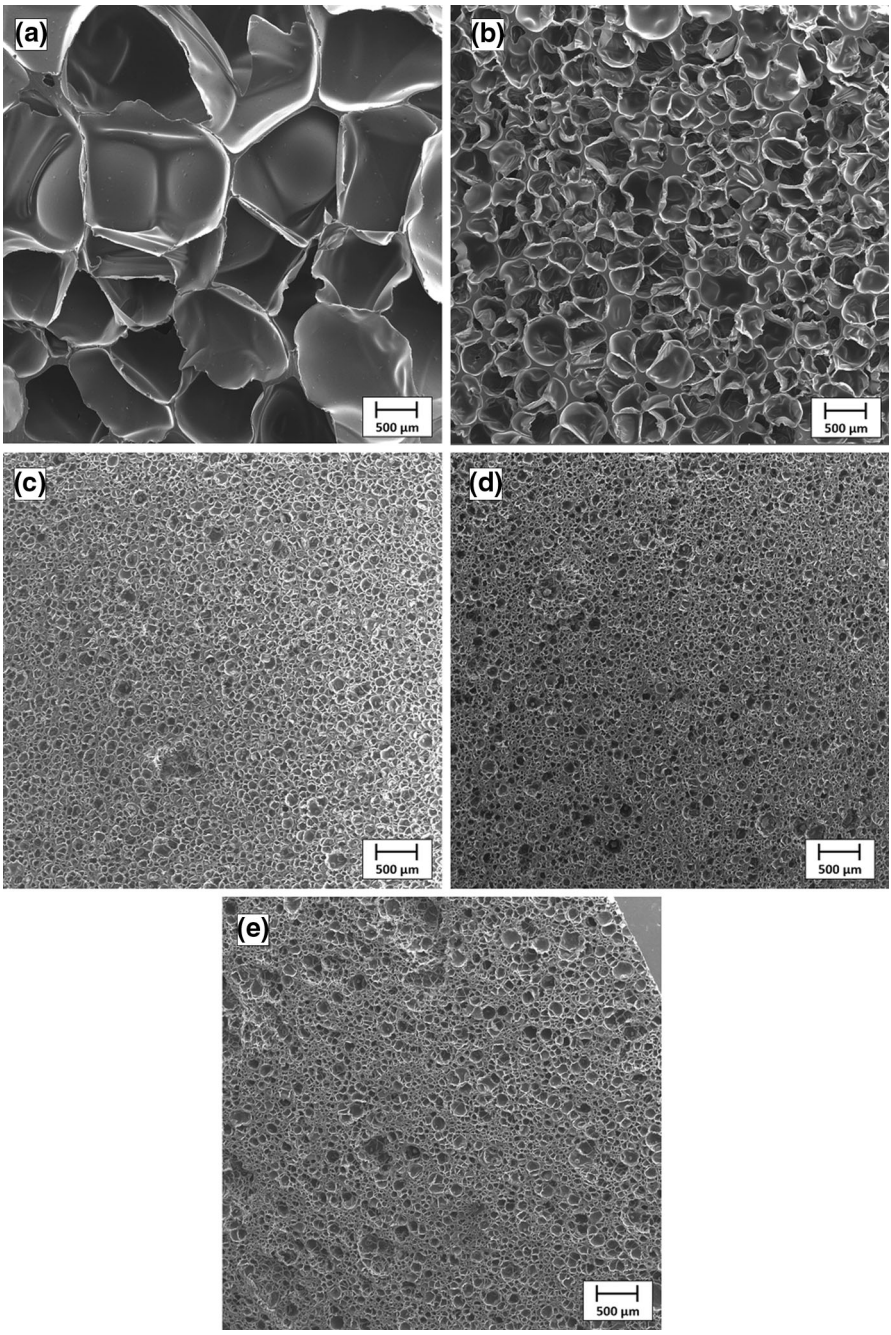

Fig. 13 SEM Microscopy of EVA.NC1% foams with pressure variation during the expansion process: **a** 1200; **b** 1800; **c** 2400; **d** 3000 and **e** 3600 psi

Table 3 Characteristics of EVA foams, reinforced with 1% of NC, produced at a constant temperature (80 °C) and pressure variation

Pressure in which the foam was produced (psi)	Foam density (g/cm^3)	Porosity (%)	Average Cell Size (μm)	Cell number per micrograph*	*Nf* (cell/cm^3)
1200	0.054 ± 0.006	94.2	1078 ± 230	21	4.16×10^6
1800	0.139 ± 0.009	85.2	334 ± 52	193	1.05×10^8
2400	0.168 ± 0.009	82.1	109 ± 47	1086	1.35×10^9
3000	0.190 ± 0.011	79.7	147 ± 52	988	1.14×10^9
3600	0.210 ± 0.010	77.0	180 ± 85	773	7.66×10^8

* SEM magnification = 100×

lower is the pressure in the system, larger is the size of the cells and the higher is the pressure, the greater is the tendency to form foams with bimodal cells and irregular sizes.

Acknowledgements The authors would like to thank the National Council of Technological and Scientific Development (CNPq) and the Secretariat of Science, Innovation and Development of Rio Grande do Sul (SCT/RS) for the financial support.

References

1. Trone JL (1996) Thermoplastics Foams. Ed. Publishing company, Sherwood
2. Eaves D (2004) Handbook of polymer Foams. Ed. Rapra Technology, UK
3. Li Q, Matuana LM (2003) Foam extrusion of high density polyethylene/wood-flour composites using chemical foaming agents. J Appl Polym Sci 88:3139–3150. doi:10.1002/app.12003
4. Bledzki AK, Faruk O (2006) Microcellular injection molded wood fiber PP composites: part I—effect of chemical foaming agent content on cell morphology and physico-mechanical properties. Cell. Plast. 41:63–76. doi:10.1177/0021955X06060945
5. Bledzki AK, Faruk O (2006) Injection Moulded microcellular wood fiber-polypropylene composites. Compos Part A-Appl. 37:1358–1367. doi:10.1016/j.compositesa.2005.08.010
6. Sauceau M, Nikitine C, Rodier E, Fages J (2007) Effect of supercritical carbon dioxide on polystyrene extrusion. J Supercrit Fluids 43:367–373. doi:10.1016/j.supflu.2007.05.014
7. Jacobs MA, Kemmere MF, Keurentjes JTF (2004) Foam processing of poly(ethylene-*co*-vinyl acetate) rubber using supercritical carbon dioxide. Polymer 45:7539–7547. doi:10.1016/j.polymer.2004.08.061
8. Rizvi GM, Park CB, Lin WS, Guo G, Iliev RP (2003) Expansion mechanism of plastic/wood-flour composites foams with moisture, dissolved gaseous volatiles and undissolved bubbles. Polym Eng Sci 43:1347–1360. doi:10.1002/pen.10115
9. Tsivintzelis I, Angelopoulou AG, Panayiotou C (2007) Foaming of polymers with supercritical CO_2: an experimental and theoretical study. Polymer 48:5928–5939. doi:10.1016/j.polymer.2007.08.004
10. Mori T, Hayashi H, Okamoto M, Yamasaki S, Hayami H (2009) Foam processing of polyethylene ionomers with supercritical CO_2. Compos Part A-Appl Sci 40:1708–1716. doi:10.1016/j.compositesa.2009.08.018
11. Zhu XH, Lee LY, Jackson JSH, Tong YW (2008) Characterization of porous poly(D, L-lactic-*co*-glycolic acid) sponges fabricated by supercritical CO_2 gas-foaming method as a scaffold for three-dimensional growth of Hep3B cells. Biotechnol Bioeng 100:998–1009. doi:10.1002/bit.21824
12. Goren K, Chen L, Schadler LS, Ozisik R (2010) Influence of nanoparticle surface chemistry and size on supercritical carbon dioxide processed nanocomposite foam morphology. J Supercrit Fluids 51:420–427. doi:10.1016/j.supflu.2009.09.007
13. Ema Y, Ikeya M, Okamoto M (2006) Foam processing and cellular structure of polylactide-based nanocomposites. Polymer 47:5350–5359. doi:10.1016/j.polymer.2006.05.050

14. Antunes M, Gedler G, Velasco JI (2013) Multifunctional nanocomposite foams based on polypropylene with carbon nanofillers. J Cell Plast 49:259–279. doi:10.1177/0021955X13477433
15. Shan CW, Izwana MI, Ghazali MI (2012) Study of flexible polyurethane foams reinforced with coir fibres and tyre particles. Int J Appl Phys Math 2:123–130. doi:10.7763/IJAPM.2012.V2.67
16. Siqueira AS, Soares BG (2006) O efeito de EPDM modificado com Grupos Mercapto ou Tioacetato na Cinética de Vulcanização de Misturas de NR/EPDM. Polímeros 16:299–304. doi:10.1590/S0104-14282006000400009
17. Peng Y, Gardner DJ, Han Y (2012) Drying cellulose nanofibrils: in search of a suitable method. Cellulose 19:91–102. doi:10.1007/s10570-011-9630-z
18. Khalil HPSA, Davoudpour Y, Islam MdN, Mustapha A, Sudesh K, Dungani R, Jawaid M (2014) Production and modification of cellulose nanofibrillated using various mechanical processes: a review. Carbohydr Polym 99:649–665. doi:10.1016/j.carbpol.2013.08.069
19. Sauders RE, Pawlak JJ, Lee JM (2014) Properties of surface acetylated microfibrillated cellulose relative to intra- and inter-fibril bonding. Cellulose 21:1541–1552. doi:10.1007/s10570-014-0177-7
20. Park CB, Baldwin DF, Suh NP (1995) Effect of the pressure drop rate on cell nucleation in continuous processing of microcellular polymers. Polym Eng Sci 35:432–440. doi:10.1002/pen.760350509
21. Jones SF, Evans GM, Galvin KP (1999) Bubble nucleation from gas cavities—a review. Adv Colloid Interface 80:27–50. doi:10.1016/S0001-8686(98)00074-8
22. Leung SNS (2009) Mechanisms of cell nucleation, growth, and coarsening in plastics foaming: theory, simulation, and experiment. PhD Thesis. Department of Mechanical and Industrial Engineering, University of Toronto
23. Spence KL, Venditti RA, Rojas OJ, Habibi Y, Pawlak JJ (2011) The effect of chemical composition on microfibrillar cellulose films from wood pulps: water interactions and physical properties for packaging applications. Cellulose 18:1097–1111. doi:10.1007/s10570-010-9424-8
24. Kalia S, Boufi S, Celli A, Kango S (2014) Nanofibrillated cellulose: surface modification and potential applications. Colloid Polym Sci 292:5–31. doi:10.1007/s00396-013-3112-9
25. Petchwattana N, Sirijutaratana C (2011) Influences of particle sizes and contents of chemical blowing agents on foaming wood plastic composite prepared from poly(vinyl chloride) and rice hull. Mater Des 32:2844–2850. doi:10.1016/j.matdes.2010.12.044
26. Matuana LM, Faruk O, Diaz CA (2009) Cell morphology of extrusion foamed poly(lactic acid) using endothermic chemical foaming agent. Bioresour Technol 100:5947–5954. doi:10.1016/j.biortech.2009.06.063
27. Sefadi JS, Luyt AS (2012) Morphology and properties of EVA/empty fruit bunch composites. J Thermoplast Compos Mater 27:895–914. doi:10.1177/0892705711421806
28. Xu ZM, Jiang XL, Liu T, Hu GH, Zhao L, Zhu ZH, Yuan WK (2007) Foaming of polypropylene with supercritical carbon dioxide. J Supercrit Fluids 41:299–310. doi:10.1016/j.supflu.2006.09.007
29. Chen L, Wang X, Straff R, Blizard K (2002) Shear stress nucleation in microcellular foaming process. Polym Eng Sci 42:1151–1158. doi:10.1002/pen.11019
30. Duan Z, Ma J, Xue C, Deng F (2014) Effect of stearic acid/organic montmorillonite on EVA/SA/OMMT nanocomposite foams by melting blending. J Cell Plast 50:263–277. doi:10.1177/0021955X14525796
31. Han JH, Han CD (1990) Bubble nucleation in polymeric liquids. II. Theoretical considerations. J Polym Sci Part B 28:743–761. doi:10.1002/polb.1990.090280510